Numerical Analysis on Seismic Response of Piled Raft Foundation with Grid-form Deep Mixing Walls Supporting a Base Isolated Building
免震建物を支持するTOFT併用パイルド・ラフト基礎の地震時シミュレーション解析

Junji Hamada　濱田　純次*1　Yoshimasa Shigeno　重野　喜政*2　Sadatomo Onimaru　鬼丸　貞友*3
Tomohiro Tanikawa　谷川　友浩*4　Naohiro Nakamura　中村　尚弘*5　Kiyoshi Yamashita　山下　清*6

Summary

The purpose of this study is to clarify the seismic performance of piled raft foundations with ground improvement based on seismic observation records. The monitored building, which is a twelve-story base-isolated structure, is located on loose silty sand underlain by soft cohesive soil in Tokyo, Japan. On March 11, 2011, when the 2011 off the Pacific Coast of Tohoku Earthquake struck the building site, the seismic response of the soil-foundation-structure system was successfully recorded during the earthquake. This paper presents a simulation analysis of the seismic behavior of the building during the earthquake using a detailed three dimensional finite-element model. The simulation results agrees well with the observed peak acceleration reduction of the superstructure created by the base-isolation system, well the bending moments on the piles induced by large ground deformation.

Keywords: the 2011 off the Pacific Coast of Tohoku Earthquake, piled raft foundation, seismic observation, simulation analysis, finite element method, grid-form ground improvement, base isolation

梗　概

本研究の目的は，地盤改良を併用したパイルド・ラフト基礎の地震時挙動を地震観測データより明らかにすることである。観測した建物は軟弱粘性土地盤上に建つ12階建て免震建物であり，2011年東北地方太平洋沖地震で地盤，基礎，上部の地震応答を記録した。本論文では詳細な3次元有限要素モデルを用いて，そのシミュレーション解析を行った。解析結果は免震装置による上部建物の応答低減や地盤変位に応じて杭曲げモーメントが発生している観測記録とよく対応した。

キーワード：2011年東北地方太平洋沖地震，パイルド・ラフト基礎，地震観測，シミュレーション解析，有限要素法，格子状地盤改良，基礎免震

1　INTRODUCTION

A seismic design concept for the piled raft foundations is important and necessary especially in highly active seismic areas such as Japan. In the last decade, shaking table tests and static lateral loading tests using centrifuge model or large scale model (Watanabe et al.[1)], Horikoshi et al.[2)], Matsumoto et al.[3)], Katzenbach & Turek[4)], Matsumoto et al.[5)], Hamada et al.[6)]) and analytical studies (Kitiyodom & Matsumoto[7)], Hamada et al.[8)]) have been carried out. Mendoza et al.[9)] reported on the static and seismic behaviour of a piled-box foundation supporting an urban bridge in Mexico City clay. The report examined the response of the soil-foundation system that was recorded during two seismic events in 1997 in which the foundation's maximum horizontal acceleration was 0.31 m/s^2. However, only a few case histories exist on the monitoring of the soil-pile-structure interaction behavior during earthquakes.

＊1　Chief Researcher, Research & Development Institute, Dr. Eng.　技術研究所　主任研究員　博士(工学)
＊2　Chief Researcher, Research & Development Institute　技術研究所　主任研究員
＊3　Osaka Main Office Building design department, Dr. Eng.　大阪本店設計部　課長　博士(工学)
＊4　Researcher, Research & Development Institute　技術研究所　研究員
＊5　Group Leader, Research & Development Institute, Dr. Eng.　技術研究所　構造部　応用数理グループ長　博士(工学)
＊6　Executive Manager, Research & Development Institute, Dr. Eng.　技術研究所　専門役　博士(工学)

The purpose of this study is to clarify the seismic performance of piled raft foundations based on seismic observation records. The monitored building, which is a twelve-story base-isolated structure, is located on loose silty sand underlain by soft cohesive soil in Tokyo, Japan. A piled raft with ground improvement was employed to cope with the liquefiable sand as well as to improve the bearing capacity of the raft foundation (Yamashita et al.[10], Yamashita et al.[11]).

On March 11, 2011, when the 2011 off the Pacific Coast of Tohoku Earthquake struck the building site, the seismic response of the soil-foundation-structure system was successfully recorded during the earthquake (Yamashita et al.[12], Hamada et al.[13], Onimaru et al.[14]). Axial force and bending moment of two piles, earth pressure and pore-water pressure beneath the raft, and accelerations of the ground and structure were measured. In this paper, the characteristics of the observed seismic motion of the ground and the building as well as the sectional forces of the piles will be discussed.

This paper presents a simulation analysis of the seismic behavior of the building during the earthquake using a detailed three dimensional finite-element model.

2 MONITORED BUILDING AND SOIL CONDITIONS

The seismically monitored building in this study is a twelve-story residential building located in Tokyo, Japan. The building is a reinforced concrete structure, 38.7 m high, with a 30.05 m by 33.25 m footprint. It has a base isolation system of laminated rubber bearings. Figure 1 shows a schematic view of the building and its foundation with typical soil profiles. The soil profile down to a depth of 7 m is fill and loose silty sand, and from 7 m to 44 m, there lies very-soft to medium silty clay strata. The silty clay between 7 to 15.5 m deep is slightly overconsolidated with an overconsolidation ratio (OCR) of about 1.5. The silty clay between 15.5 to 44 m deep is overconsolidated with OCR of 2.0 or higher. The subsoil consists of an alluvial stratum to a depth of 44 m, underlain by a diluvial sand and gravel layer of SPT N-values of 60 or higher. The ground water table appears approximately 1.8 m below the ground surface. The shear wave velocities derived from a P-S logging system were 110 to 220 m/s between 4.8 and 43 m deep, and 410 to 610 m/s in the dense sand and gravel layers below 48 m deep.

The piled raft foundation design was described in a previous paper (Yamashita et al.[11]). The average contact pressure over the raft was 199 kPa. To improve the bearing capacity of the subsoil beneath the raft, as well as to cope with the liquefiable

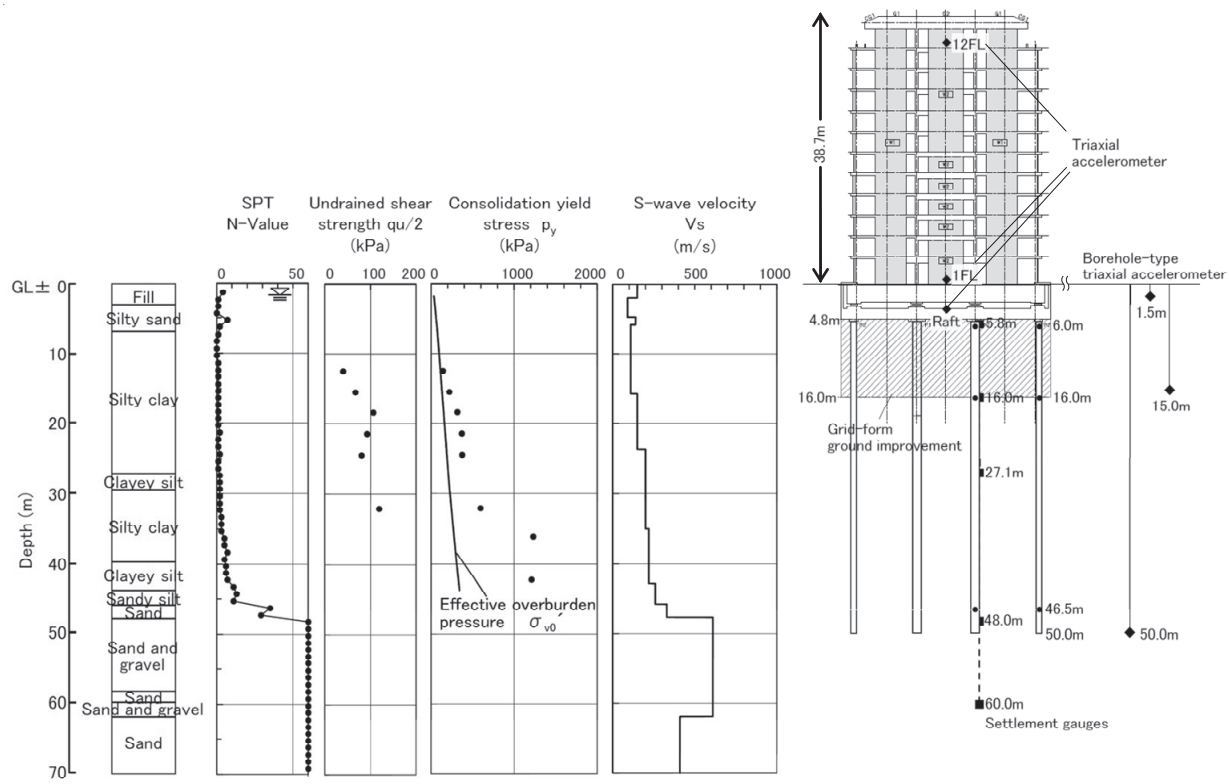

Fig. 1 Schematic view of building and foundation with soil profile

silty sand, the grid-form deep cement mixing walls were embedded in the overconsolidated silty clay that had an undrained shear strength of 75 kPa below a depth of 16 m. Consequently, a piled raft consisting of sixteen 45-m long bored precast concrete piles with diameters of 0.8 to 1.2 m (SC piles in the top portion, PHC piles in other portions) were employed. Figure 2 shows the layout of the piles and the grid-form deep cement mixing walls.

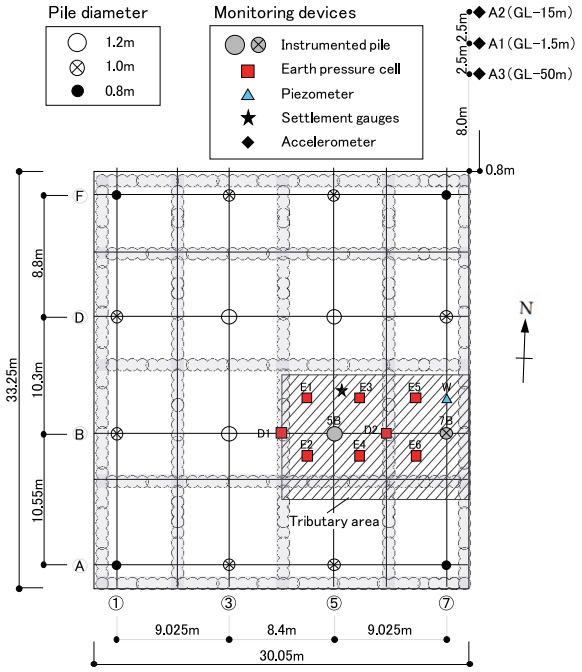

Fig. 2 Layout of piles and grid-form deep cement mixing walls with locations of monitoring devices

3 SIMULATION ANALYSIS OF OBSERVED SEISMIC RECORDS

The ground, the piles and the grid-form improved ground were modelled in as much detail as possible using a three-dimensional finite element method (FEM) and conducted simulation analysis for the 2011 off the Pacific Coast of Tohoku Earthquake.

3.1 Three dimensional finite element model

The model mesh is divided finely around the foundation as shown in Figure 3. The lateral boundaries are cyclic boundaries while the bottom boundary is a viscous boundary. There are about 210,000 elements, with about 660,000 degrees of freedom. The numerical analysis code is the in-house program called MuDIAN. The analysis is carried out in parallel with 8 threads.

3.1.1 Modelling of ground

The shear wave velocity, Vs, distribution in the ground layer is obtained by employing an optimization method in which the cost function is the error of the transfer function. Records of small earthquakes that occured before the 2011 off the Pacific Coast of Tohoku Earthquake were used in the optimization. The P-S logging results were used as the initial Vs distribution.

The equivalent linear stiffness and damping of the soils are calculated using one-dimensional equivalent linear analysis considering the nonlinear characteristics of the soils, which were obtained from cyclic triaxial tests of the samples. Figure 4 shows the shear strain dependency characteristics of each soil layer at this site, (G/G_0-γ and h-γ). The EW and NS waves of GL-50m observed during the 2011 off the Pacific Coast of Tohoku Earthquake are used as input. The analysis shows that stiffness reduction was greater for the EW input waves than for NS waves. This reduced stiffness and damping are used as the equivalent stiffness and damping in the three-dimensional analysis. Figure 5 shows the distribution of the equivalent shear velocity by depth.

3.1.2 Modelling of piles and grid-form ground improvement

The piles are modeled as the beam elements considering their volume, as shown in Fig. 3(b). The beam nodes and the ground nodes on the circumference of the piles are joined by rigid bars. The grid-form ground improvements are modeled with solid elements as shown in Fig. 3(c). They are divided finely enough in the thickness direction to prevent shear locking. The shear modulus of the ground improvements is set at 700 MPa (ρ=2.0 t/m^3, Vs=592 m/s) according to the 28-day strength of the samples. The material characteristics of the improved soil and piles are shown in Tables 1 and 2, respectively.

3.1.3 Modelling of base-isolation system

For the base-isolation, bilinear-type spring elements were employed to model horizontal characteristics and linear-type spring were employed for vertical characteristics. These models are same as those used in structural design.

3.1.4 Modelling of building

In order to match the actual layout of the design drawings, the columns were modelled using beam elements and earthquake-resistant walls and the floors were modelled using shell elements. Since the building's behavior is unlikely to become non-linear at the seismic excitation level to which the base isolation system will be subjected, linearity was assumed for the materials. The natural period when the first floor is fixed in the model agree well with the actual measurements. The damping ratio of the building is 2%.

3.2 Input seismic motion

The upward transmitting wave at a depth of 75 m, which was set as the bottom depth of the three-dimensional FEM model, was calculated using one-dimensional equivalent linear analysis and was input to the bottom of the three-dimensional model. The EW and NS waves were input together in the three-dimensional analysis.

Table 1 Characteristics of material of improved soil

Thickness (m)	Shear modulus (MN/m^2)	Poisson's ratio	Damping (%)
0.8	700	0.28	2.0

Table 2 Characteristics of material of piles

Pile diameter (mm)	Young's modulus (MN/m^2)	Damping (%)	A_e of SC pile (m^2)	I_e of SC pile (m^4)	A_e of PHC pile (m^2)	I_e of PHC pile (m^4)
800	40000	2.0	0.3268	0.02199	0.2441	0.01455
1000	40000	2.0	0.4649	0.04899	0.3633	0.03437
1200	40000	2.0	0.6714	0.10316	0.5054	0.06958

A_e : Equivalent cross-sectional area
I_e : Equivalent moment of inertia of area

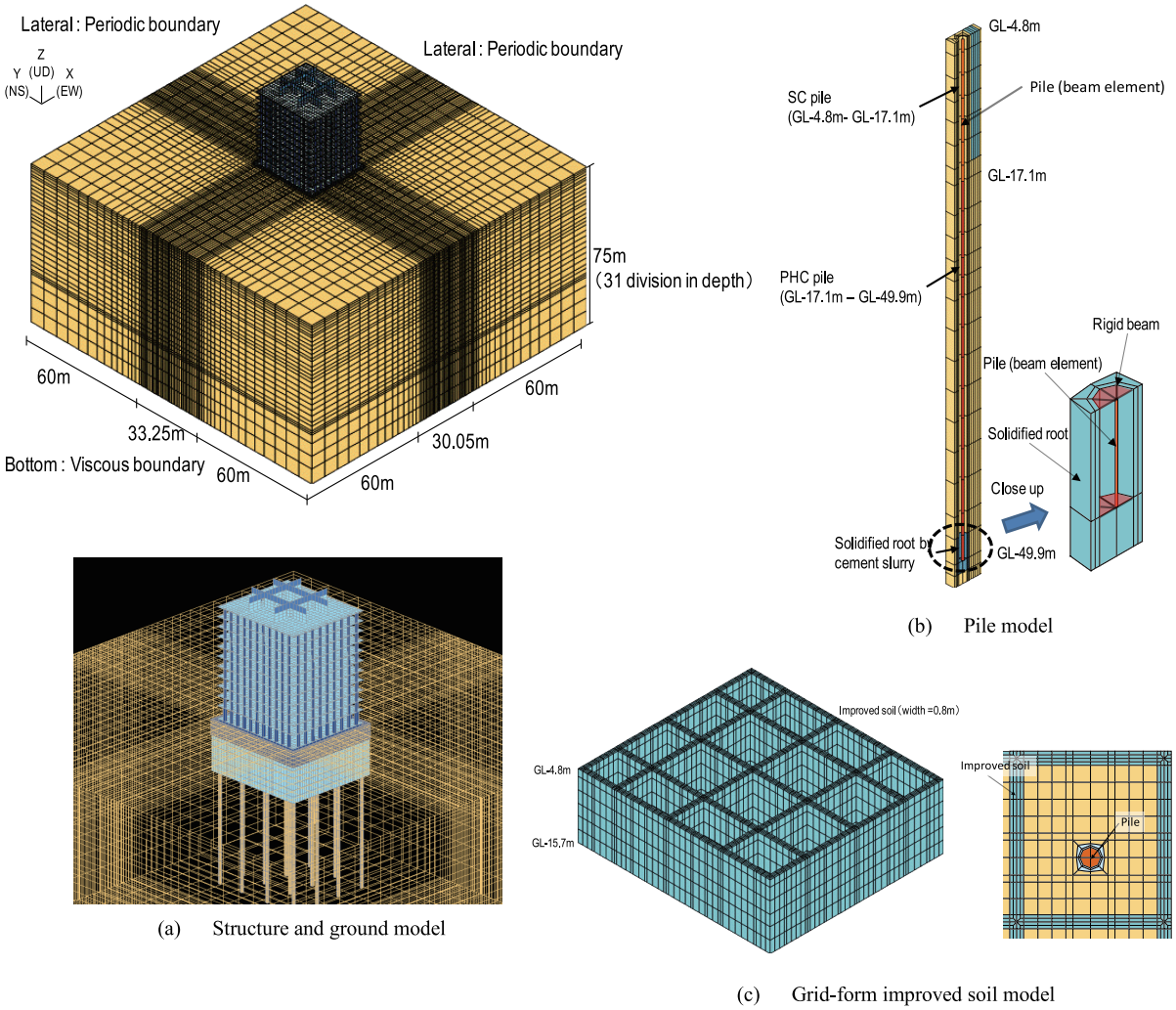

(a) Structure and ground model

(b) Pile model

(c) Grid-form improved soil model

Fig. 3 Analytical model

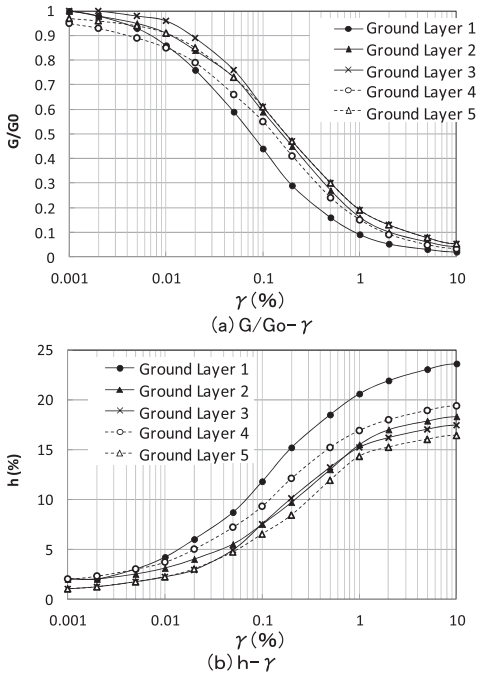

Fig. 4 Variation of shear modulus and damping ratio vs. shear strain

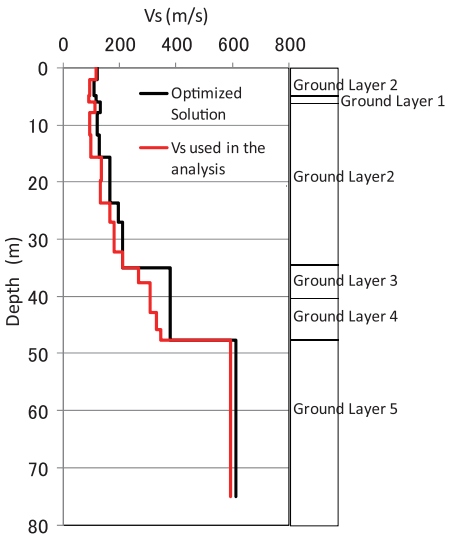

Fig. 5 Profile of optimized shear-wave velocity

4 RESULTS OF SIMULATION ANALYSIS

4.1 Seismic response of superstructure and ground

Figure 6 shows maximum acceleration profiles for the superstructure. The analytical results have slightly larger maximum accelerations in the NS direction than the observed values but they agree very well. Figures 7 and 8 show the acceleration response spectra for the analysis at the Pit and the 12th floor (12F) respectively, compared with the observed record. The analytical results at the Pit agree well with the observed record, but at the 12th floor (12F), the primary mode of the analysis accords well with the observations, but slight difference is observed in second mode (0.3~0.6 s).

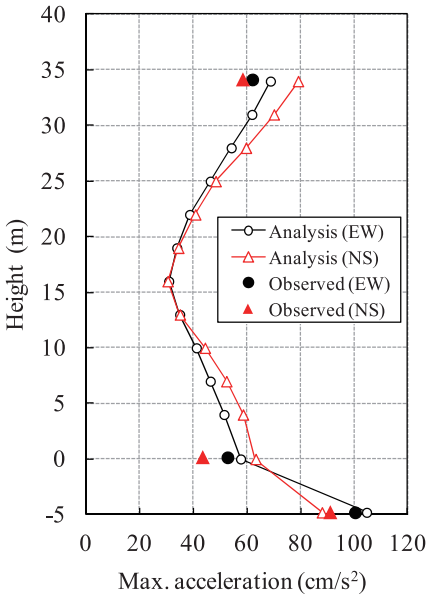

Fig. 6 Profile of maximum acceleration of superstructure

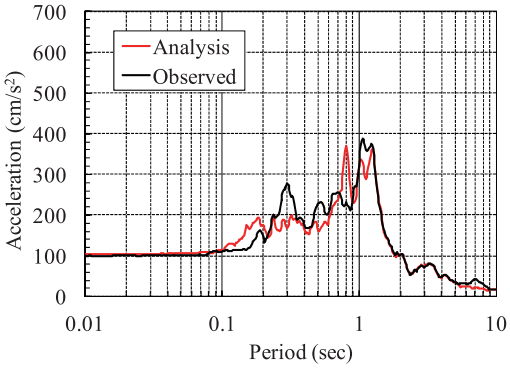

Fig. 7 Acceleration response spectrum at Pit

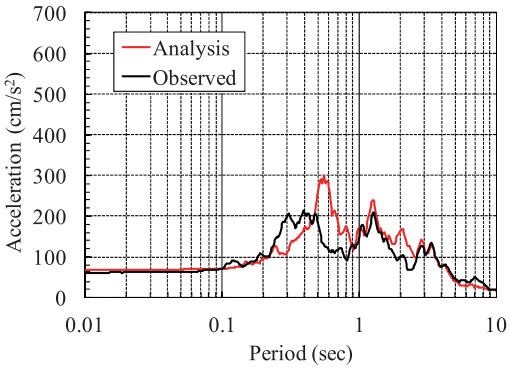

Fig. 8 Acceleration response spectrum at 12F

Figure 9 shows the time histories of the simulated ground and structure accelerations compared to observed values during 100 to 120 second, the time frame which includes the main shock. Figure 10 shows the time histories of the simulated relative displacements of the ground and the structures compared to observed values. The horizontal displacements were calculated by integrating the acceleration records, where components of the period longer than 20 s and shorter than 0.05 s were cut off. The relative displacements are calculated from GL-50m. Figure 11 shows the peak accelerations and peak relative displacements profile for the simulation and observations. The response calculated in the simulation for ground (GL-1.5m, -15m) and the Pit agree very well with the observations even though the ground was modeled using equivalent linear behavior. The analyzed superstructure response at the first floor (1F) and 12th floor (12F) slightly differ from the observations, however the analysis correctly expresses the acceleration reduction and displacement increase by the base isolation.

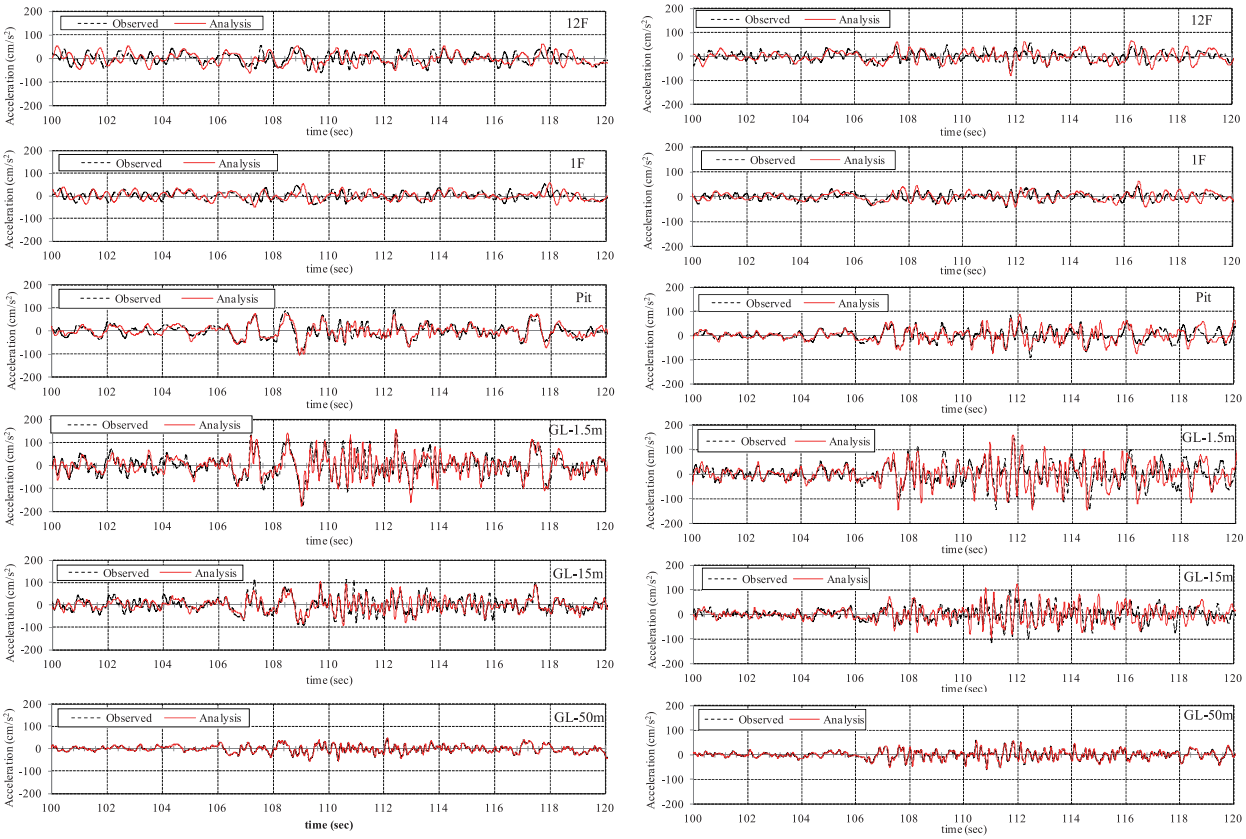

(a) EW-direction (b) NS-direction

Fig. 9 Comparison of observed and simulated acceleration time histories

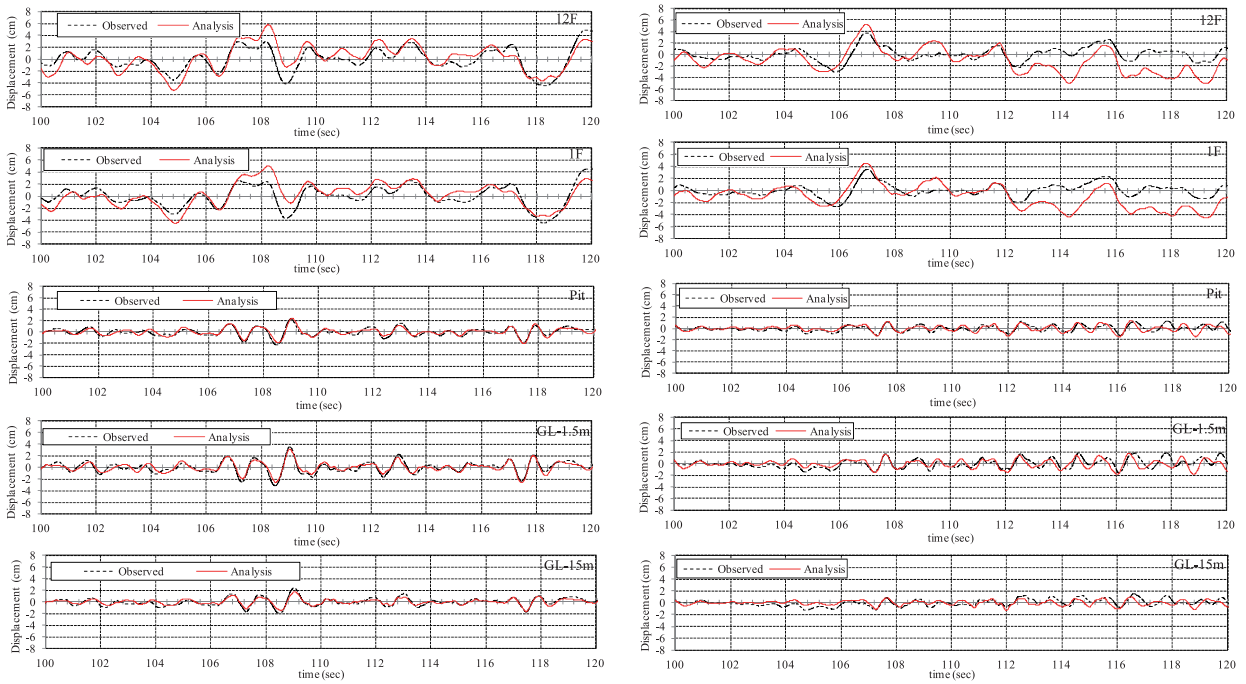

(a) EW-direction (b) NS-direction

Fig. 10 Comparison of observed and simulated time histories of relative displacements

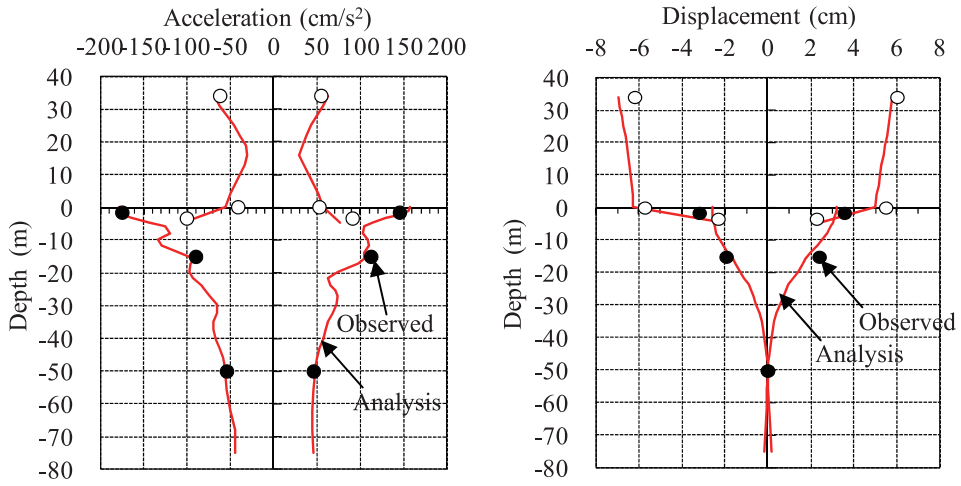

Fig. 11 Comparison of observed and simulated peak acceleration and relative displacement (EW-direction)

Figure 12 shows the Fourier spectrum ratios of "GL-1.5m to GL-50m" and "Pit to GL-1.5m". The amplitudes of the spectral ratios are smoothed using a Parzen window of bandwidth of 0.05 Hz. The spectral ratio and phase by simulations show the same tendencies as the observated data. The simulation corresponds very well not only with the observed primary natural frequency of the ground near 1 s, but also with the second and the third natural frequencies. In addition, the input loss (Pit/GL-1.5m), which is between 1 to 2 Hz, is simulated well. The input motion is reduced by ground improvement.

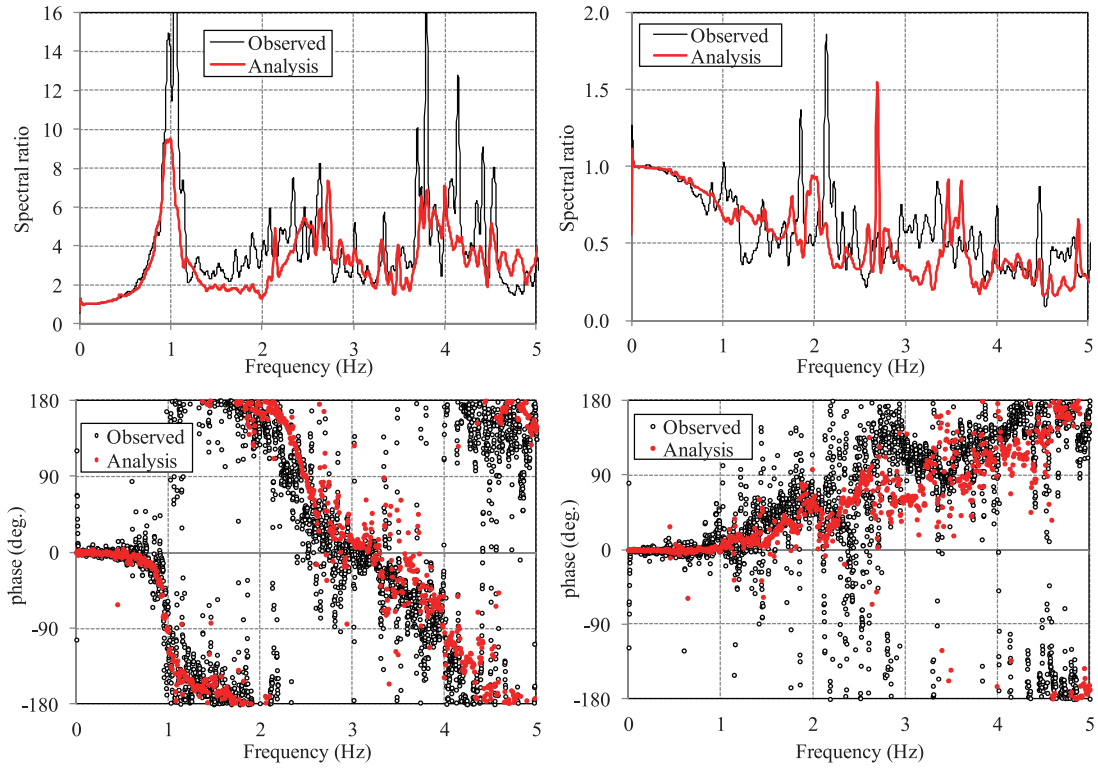

(a) GL-1.5m /GL-50m (b) Pit /GL-1.5m

Fig. 12 Comparison of observed and simulated distributions of Fourier spectrum ratios (EW-direction)

4.2 Bending moment of piles

Figure 13 shows the time histories of the incremental bending moments of the simulated piles compared to the observed values during 100 to 120 second. The analytical results are in good agreement with the observations, which indicate the same phase bending moments both at the lower end of TOFT (GL-16m) and near the pile head (GL-6m). Figure 14 compares the simulated and observed distribution of the peak bending moment of the piles. The analytical results show the same tendency as the observations in that the maximum moment near the head of pile 5B is larger than in the middle of pile 5B. It also shows the tendency for the maximum moment near the head of pile 7B to be smaller than in its middle. The observed EW moment at pile head in 7B gradually shifts to a positive value after 109 second. This tendency could not be reproduced with employed equivalent linear analysis model.

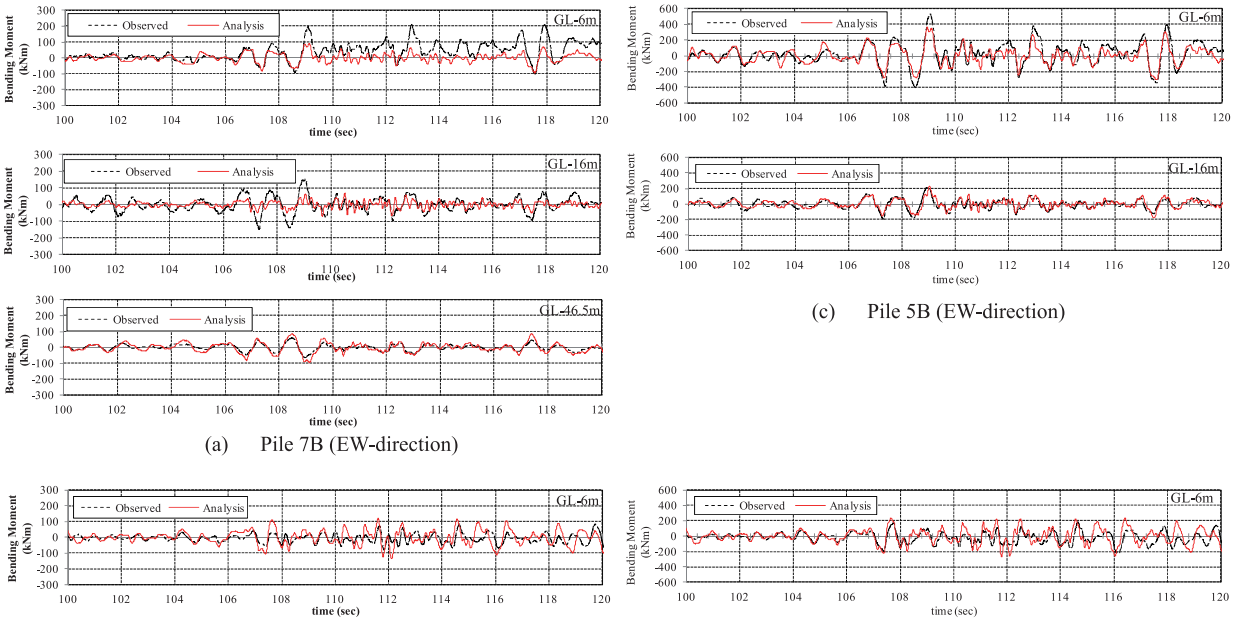

(a) Pile 7B (EW-direction)

(b) Pile 7B (NS-direction)

(c) Pile 5B (EW-direction)

(d) Pile 5B (NS-direction)

Fig. 13 Comparison of observed and simulated bending moment time histories

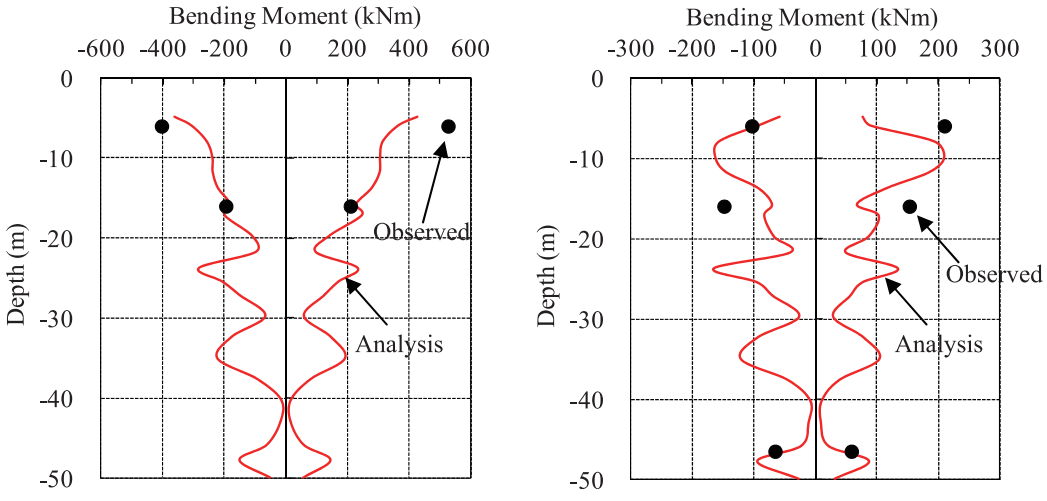

(a) Pile 5B

(b) Pile 7B

Fig. 14 Comparison of observed and simulated distributions of peak bending moment (EW-direction)

5 EFFECT OF INERTIAL FORCE AND GROUND DISPLACEMENT ON PILE BENDING MOMENT

Figure 15 compares the simulated and observed differences between the horizontal displacements near the ground surface (relative to 50 m deep) plotted against the incremental bending moments at the head of pile 5B. The analysis agrees well with the observations. The bending moments at the pile head tend to increase as the relative horizontal displacements increase in both directions. The relative EW displacement is larger than NS direction. The EW bending moment is larger than the NS bending moment corresponding to the same relative displacement.

Figure 16 compares the simulated and observed inertial force of the building versus the incremental bending moments at pile head. The inertial force of the building was estimated by multiplying the building weight by observed and analysed accelerations at the Pit, the first and the twelfth floors. The weights of the superstructure above the isolators and the substructure under the isolators are 152 and 41 MN, respectively. The analytical results also show good agreement with the observations. The effect of the inertial force on the bending moment at the pile head was not significant compared to the ground deformation.

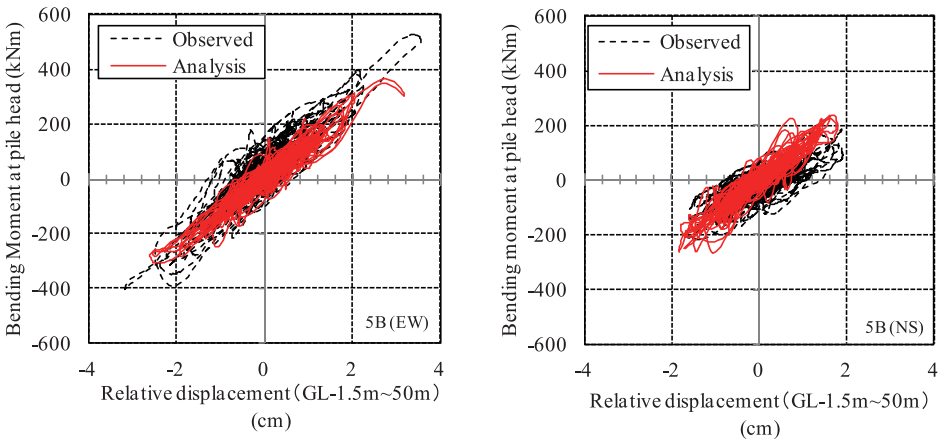

(a) Pile 5B (EW-direction) (b) Pile 5B (NS-direction)

Fig. 15 Comparison of observed and simulated relative ground displacements vs. bending moments at pile head

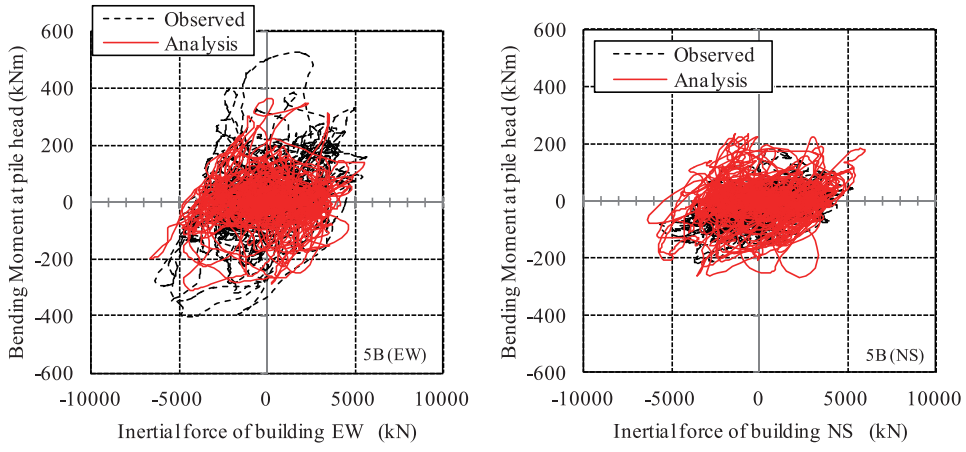

(a) Pile 5B (EW-direction) (b) Pile 5B (NS-direction)

Fig. 16 Comparison of observed and simulated inertial force of building vs. bending moments at pile head

6 CONCLUSUIONS

Simulation analysis of the seismic performance of piled raft foundation with grid-form ground improvements supporting a base-isolated building, during the 2011 off the Pacific Coast of Tohoku Earthquake, was conducted using a detailed three-dimensional finite-element model. The simulation results agreed well with the observed peak acceleration reduction of the superstructure created by the base isolation system. The simulation also showed that the peak acceleration reduction on the raft was about 60% of that at the ground surface at the building site. The reduction of the input motion appears to have been caused by the ground improvement.

The analysis and observations showed that the bending moments near the pile head and at intermediate depth, where is at the lower end of the grid-form deep cement mixing walls, behaved very similarly. In addition, the bending moments at the pile head and those at the intermediate depth increased during large ground deformations despite the inertial force of building not being significant.

REFERENCES

1）Watanabe, T., Fukuyama, H., Horikoshi, K. and Matsumoto, T. (2001): Centrifuge modeling of piled raft foundations subjected to horizontal loads, Proc. 5th Int. Conf. On Deep Foundation Practice incorporating Piletalk Int., 371-378.

2）Horikoshi, K., Matsumoto, T., Hashizume, Y., Watanabe, T. and Fukuyama, H. (2003): Performance of piled raft foundations subjected to static horizontal loads, International Journal of Physical Modelling in Geotechnics, 3(2), 37-50.

3）Matsumoto, T., Fukumura, K., Kitiyodom, P., Horikoshi, K. and Oki, A. (2004): Experimental and analytical study on behaviour of model piled rafts in sand subjected to horizontal and moment loading, International Journal of Physical Modeling in Geotechnics, 4(3), 1-19.

4）Katzenbach, R. and Turek, J. (2005): Combined pile-raft foundation subjected to lateral loads, Proc. 16th Int. Conf. On Soil Mechanics and Geotechnical Engineering, 2001-2004.

5）Matsumoto, T., Nemoto, H., Mikami, H., Yaegashi, K., Arai, T. and Kitiyodom, P. (2010): Load tests of piled raft models with different pile head connection conditions and their analyses, Soils and Foundations, Vol.50, No.50, 63-81.

6）Hamada, J., Tsuchiya, T., Tanikawa, T. and Yamashita, K. (2011): Lateral loading tests on piled raft foundations at large scale and their analyses, International Conference on Advances in Geotechnical Engineering, Nov.7-9, 1059-1064.

7）Kitiyodom, P. and Matsumoto, T. (2003): A simplified analysis method for piled raft foundations in non-homogeneous soils, Int. J. Numer. Anal. Meth. Geomech., 85-109.

8）Hamada, J., Tsuchiya, T. and Yamashita, K. (2009): Theoretical equations to evaluate the stress of piles on piled raft foundation during earthquake, J. Structural Const. Eng. (AIJ), Vol. 74, No. 644, 1759-1767 (in Japanese).

9）Mendoza, M. J., Romo, M. P., Orozco, M. and Dominguez, L. (2000): Static and seismic behavior of a friction pile-box foundation in Mexico City clay, Soils & Foundations, Vol.40, No.4, 143-154.

10）Yamashita, K., Yamada, T. and Hamada, J. (2011a): Investigation of settlement and load sharing on piled rafts by monitoring full-scale structures, Soils & Foundations, Vol.51, No.3, 513-532.

11）Yamashita, K., Hamada, J. and Yamada, T. (2011b): Field measurements on piled rafts with grid-form deep mixing walls on soft ground, Geotechnical Engineering Journal of the SEAGS & AGSSEA, Vol.42, No.2, 1-10.

12）Yamashita, K., Hamada, J., Onimaru, S. and Higashino, M. (2012): Seismic behavior of piled raft with ground improvement supporting a base-isolated building on soft ground in Tokyo, Soils & Foundations, Special Issue on Geotechnical Aspects of the 2011 off the Pacific Coast of Tohoku Earthquake, Vol.52, No.5, 1000-1015.

13）Hamada, J., Tanikawa, T., Onimaru, S. and Yamashita, K. (2 0 1 2): Seismic observations on piled raft foundation with ground improvement supporting a base-isolated building, 15thWCEE.

14）Onimaru, S., Hamada, J., Nakamura, N. and Yamashita, K. (2012): Dynamic soil-structure interaction of a building supported by piled raft and ground improvement during the 2011 Tohoku Earthquake, 15thWCEE.